Biochimica et Biophysica Acta 1853 (2015) 2481–2491

Contents lists available at ScienceDirect

Biochimica et Biophysica Acta

journal homepage: www.elsevier.com/locate/bbamcr

Identification of lipid droplet structure-like/resident proteins in *Caenorhabditis elegans*

Huimin Na [a,b,1], Peng Zhang [a,b,1], Yong Chen [a], Xiaotong Zhu [a,b], Yi Liu [a], Yangli Liu [a,b], Kang Xie [a,b], Ningyi Xu [c,d], Fuquan Yang [a], Yong Yu [e], Simon Cichello [f], Ho Yi Mak [c,d], Meng C. Wang [e], Hong Zhang [a], Pingsheng Liu [a,*]

[a] National Laboratory of Biomacromolecules, Institute of Biophysics, Chinese Academy of Sciences, Beijing 100101, China
[b] University of Chinese Academy of Sciences, Beijing 100049, China
[c] Stowers Institute for Medical Research, Kansas City, MO 64110, USA
[d] Department of Molecular and Integrative Physiology, University of Kansas Medical Center, Kansas City, KS 66160, USA
[e] Department of Molecular and Human Genetics Huffington Center on Aging, Baylor College of Medicine, Houston, TX 77030, USA
[f] School of Life Sciences, La Trobe University, Melbourne, Victoria 3086, Australia

ARTICLE INFO

Article history:
Received 2 March 2015
Received in revised form 17 May 2015
Accepted 19 May 2015
Available online 27 May 2015

Keywords:
Lipid droplet
Structure-like/Resident Proteins
Triacylglycerol (TAG)
MDT-28
Perilipin family

ABSTRACT

The lipid droplet (LD) is a cellular organelle that stores neutral lipids in cells and has been linked with metabolic disorders. *Caenorhabditis elegans* has many characteristics which make it an excellent animal model for studying LDs. However, unlike in mammalian cells, no LD structure-like/resident proteins have been identified in *C. elegans*, which has limited the utility of this model for the study of lipid storage and metabolism. Herein based on three lines of evidence, we identified that MDT-28 and DHS-3 previously identified in *C. elegans* LD proteome were two LD structure-like/resident proteins. First, MDT-28 and DHS-3 were found to be the two most abundant LD proteins in the worm. Second, the proteins were specifically localized to LDs and we identified the domains responsible for this targeting in both proteins. Third and most importantly, the depletion of MDT-28 induced LD clustering while DHS-3 deletion reduced triacylglycerol content (TAG). We further characterized the proteins finding that MDT-28 was ubiquitously expressed in the intestine, muscle, hypodermis, and embryos, whereas DHS-3 was expressed mainly in intestinal cells. Together, these two LD structure-like/resident proteins provide a basis for future mechanistic studies into the dynamics and functions of LDs in *C. elegans*.

1. Introduction

The current upswing in research interest in lipid droplets (LDs) has been fueled by their connection to human metabolic disorders, the importance of neutral lipids in food products, and the development of biofuels [1–5]. LDs have been found in almost all organisms from bacteria to mammals and throughout most cell types in multicellular organisms [5,6]. LDs are a cellular organelle that consists of a neutral lipid core covered with a monolayer phospholipid membrane and proteins. The core contains triacylglycerol (TAG), cholesterol esters, and ether lipids [7]. LD-associated proteins have been identified in many species, from bacteria to humans [5], and can be categorized into four groups: LD structure-like/resident, lipid synthetic and metabolic, membrane traffic, and cell signaling proteins [8]. Perilipin [9] and adipose differentiation-related protein (ADRP) [10,11] are considered LD structure-like/resident proteins. They belong to the Perilipin family (PLINs), which includes three other members: Tip47 [12], S3-12 [13] and OXPAT [14]. PLIN family proteins are only expressed in mammals and *Drosophila*[15].

Further, LDs have been observed to be closely linked both at a molecular level of communication and also proximity to endoplasmic reticulum [16,17], early endosomes [18], mitochondria [19], peroxisome [20], and other cellular organelles [21], implying a possible role for LDs in energy metabolism regulation and intracellular lipid trafficking. Although LDs are an important cellular organelle and its research has significant progresses in last decade, the mechanisms behind LD formation, morphological changes and functions remain elusive.

LDs have been studied in many organisms, providing opportunities for comparative analyses. Among them *C. elegans* stands out as an excellent animal model, not only due to the ease of genetic manipulation and visualization, but also because of the demonstrated linkages between fat storage, metabolism, reproduction, and the animal's lifespan [22–26]. Our previous study provided a shotgun proteome and identified a LD marker protein DHS-3. However, the utility of this animal model for LD research has been limited due to a lack of knowledge regarding LD structure-like/resident proteins [25,27,28].

Following up on our previous study where we identified a LD marker protein, DHS-3, in *C. elegans*[29], we have performed a comprehensive

* Corresponding author. Tel./fax: +86 10 64888517.
E-mail address: pliu@ibp.ac.cn (P. Liu).
[1] These authors contributed equally to this work.

http://dx.doi.org/10.1016/j.bbamcr.2015.05.020
0167-4889/

proteomic study of LDs isolated from *C. elegans*. We have identified two major LD proteins in the animal, MDT-28 and DHS-3. Both proteins were localized to LDs by fluorescence microscopy. DHS-3 was only expressed in the intestine, whereas MDT-28 was located in most tissues. We used mutational analysis to identify the regions of the proteins responsible for LD targeting. Finally, we demonstrated that the depletion of MDT-28 induces LD clustering while DHS-3 deletion reduces TAG. These data indicate that MDT-28 and DHS-3 are two LD structure-like/resident proteins in the worm, which will facilitate the study of LDs and lipid metabolism in this important animal model.

2. Materials and methods

2.1. Strains and culture conditions

The N2 Bristol strain of *C. elegans* was used as wild type in this study. The *dhs-3*(gk873395) worm was provided by the *Caenorbhabditis* Genetics Center (CGC) at the University of Minnesota. The *mdt-28*(*tm1704*) and *F22F7.1*(*tm5652*) worms were provided by National BioResource Project (NBRP). The *Pdhs-3::dhs-3::GFP*, *Pmdt-28::mdt-28::mCherry*, and *PF22F7.1::F22F7.1::GFP* worms were constructed in our laboratory. Strains *Pvha-6::dhs-3::GFP* (single copy) and *Pmdt-28::mdt-28::mRuby* (single copy) were generated by professor Ho Yi Mak. Muscle and hypodermis specific expression markers *Pmyo-3::GFP* and *Pceh-14::GFP* were crossed with *Pmdt-28::mdt-28::mCherry* to illuminate the tissue distribution of MDT-28. The *Pvha-6::dhs-3::GFP, mdt-28, Pvha-6::dhs-3::GFP, F22F7.1, Pvha-6::dhs-3::GFP, mdt-28, and F22F7.1* strains were prepared by our laboratory for the *mdt-28* and *F22F7.1* phenotype study. All worms were maintained on agar plates seeded with an OP50 bacterial lawn using a standard protocol.

The CHO K2 cell line was cultured by a method described previously [30] and used for the DHS-3 and MDT-28 lipid droplet targeting experiment.

2.2. Isolation of lipid droplets

LDs were isolated by the method previously described [29,31]. First, about 4×10^5 young adults were harvested and washed with Phosphate Buffered Saline (PBS)/0.001% Triton-X100 and suspended in 20 ml buffer A (25 mM Tricine, pH 7.6, 250 mM sucrose, and 0.2 mM phenylmethylsulfonylfluoride), followed by homogenization using a Polytron (Cole-Parmer® Labgen™ 125 and 700 Tissue Homogenizers). The homogenate was centrifuged at 1000 *g* for 30 s. The supernatant was homogenized again by nitrogen cavitation (Ashcroft Duralife Pressure Gauge) after a 15 min, 750 pounds per square inch (PSI) incubation on ice, and was then centrifuged at 1000 *g* for 10 min. 9 ml of post-nuclear supernatant (PNS), was collected and loaded into an SW40 tube. The homogenate was overlaid with 3 ml of buffer B (20 mM HEPES, pH 7.4, 100 mM KCl, and 2 mM $MgCl_2$) and was centrifuged at 12,628 *g* for 1 h at 4 °C. The LD fraction was carefully collected from top layer of the gradient and washed with 200 μl buffer B 3 times. For embryonic LD isolation, the embryos were harvested using a bleach method [32]. Briefly, 4×10^5 3–4 day old adults were collected into a 15 ml tube and resuspended in a 7 ml of ddH_2O. 1 ml of 5 N NaOH and 2 ml of bleach buffer (5% solution of sodium hypochlorite) were added and then vortexed briefly. The sample was incubated at room temperature until the worms dissolved (usually 5–8 min). The sample was then centrifuged for 1 min at 1500 *g*. The supernatant was discarded and the pellet was washed 5 times. The same LD isolation procedure described above was then carried out, starting with the nitrogen cavitation.

2.3. Protein preparation and Western blot

Proteins were precipitated using 100% acetone, and were collected by centrifugation at 20,000 *g* for 10 min. Protein pellets were dissolved in 2 × SDS sample buffer at a final concentration of about 1 mg/ml for

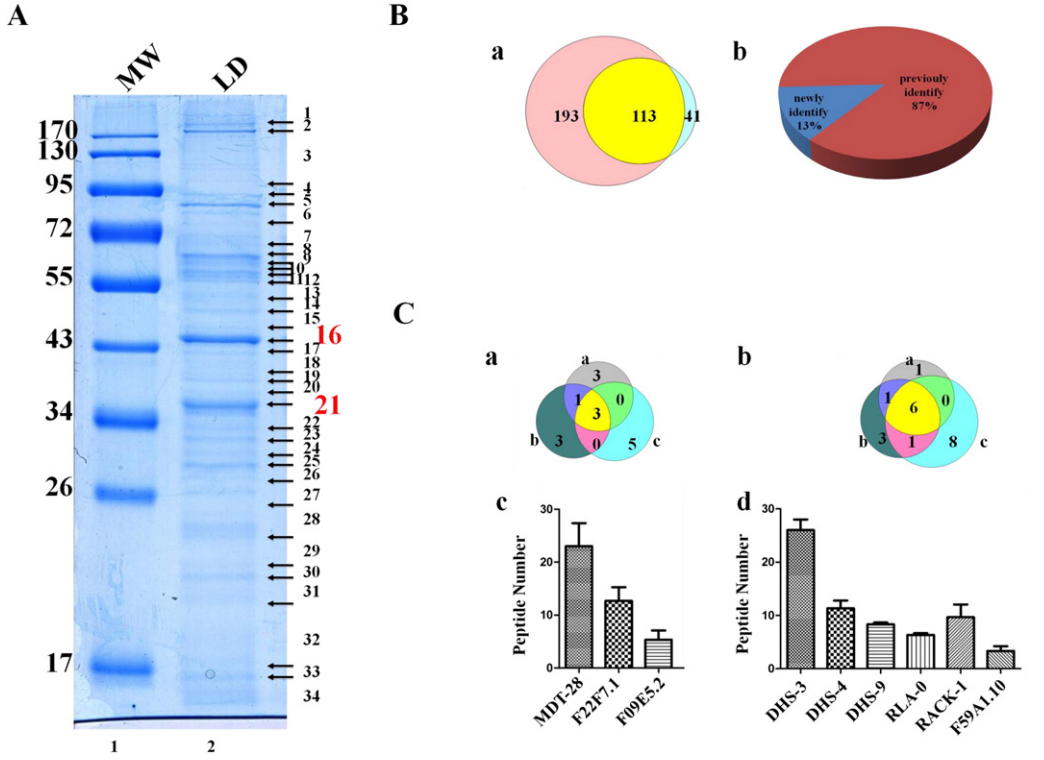

Fig. 1. Proteomic analyses of *C. elegans* lipid droplets. A. LDs were isolated from wild type adult animals, the proteins were separated by SDS-PAGE, and were stained using Colloidal blue. The LD lane was sliced into 34 pieces (arrow indicate cutting sites) and subjected to mass spectrometry protein identification as described previously [30]. B. (a) The current proteome was compared with previous LD proteomes of *C. elegans* using a Venn diagram. (b) The current proteome was compared with previous proteomic studies of the species reported except *C. elegans*. C. Proteins of the two major bands; band 16 (a) and band 21 (b) from three independent LD isolations and proteomic analyses are shown in two Venn diagrams. Peptide numbers for proteins identified in band 16 (c) and band 21 (d) are represented in the bar graphs.

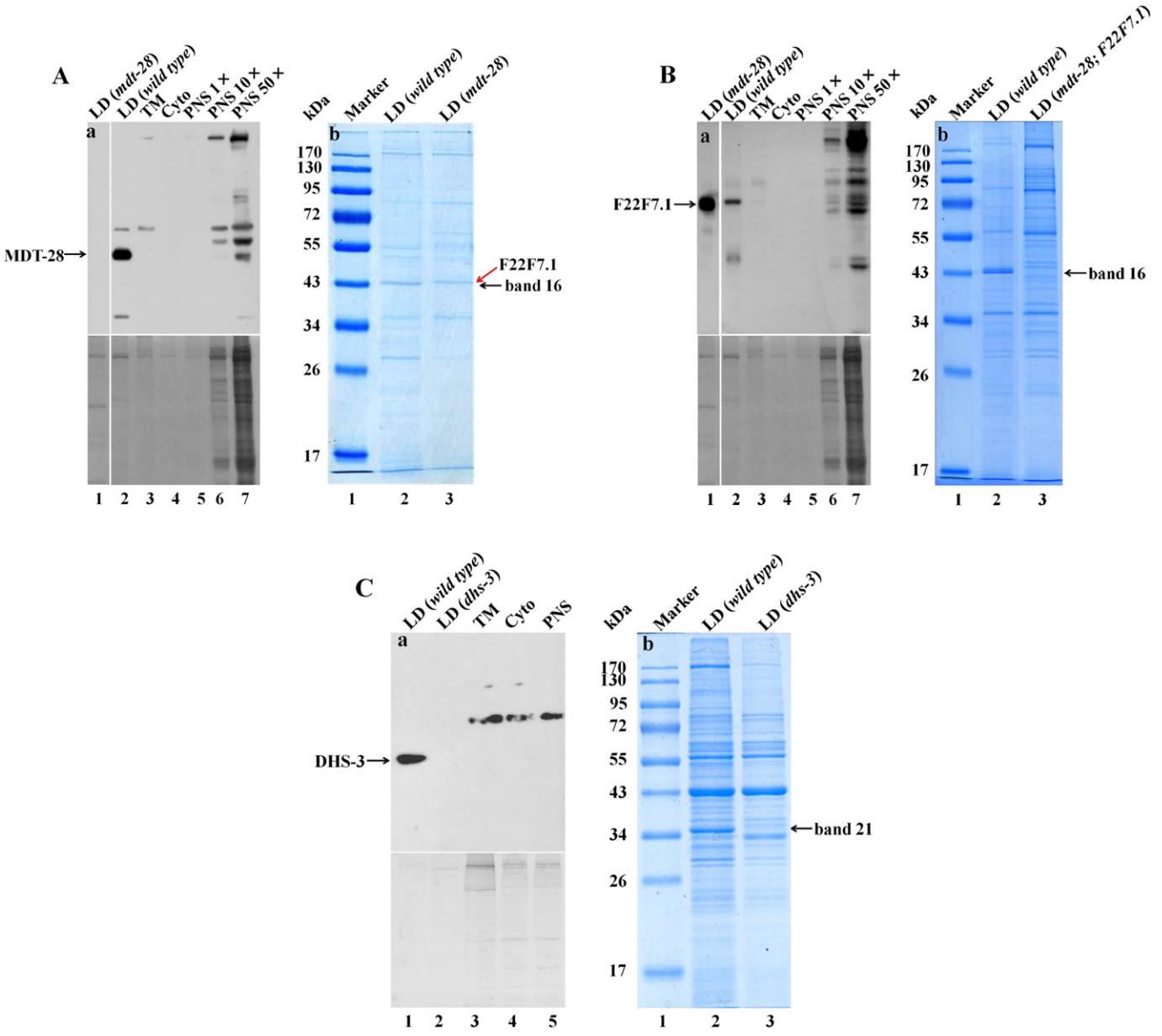

Fig. 2. Identification of lipid droplet abundant proteins. The deletion mutants of *mdt-28* and *dhs-3* were obtained, and the deletion mutant of *F22F7.1* and double mutant of *mdt-28* and *F22F7.1* were generated. LDs were isolated from all these mutants and wild type. The LD proteins were extracted and subjected to Colloidal blue staining and Western blot. A. a) MDT-28 was examined in LD, total membrane (TM), cytosol (Cyto), and postnuclear supernatant (PNS) of wild type and in LD of *mdt-28* deletion mutant using Western blot with anti-MDT-28 (upper panel). Arrow points MDT-28 band. Protein loading was detected by Coomassie blue staining (lower panel). b) LD proteins were compared between wild type and *mdt-28* deletion mutant using Colloidal blue staining. Band 16 is pointed by a black arrow and a new band is pointed by a red arrow. B. a) F22F7.1 was examined in four fractions of wild type and in LD of *mdt-28* deletion mutant using Western blot with anti-F22F7.1 (upper panel). Arrow points F22F7.1 band. Protein loading was detected by Coomassie blue staining (lower panel). b) LD proteins were compared between wild type and double mutant of *mdt-28* and *F22F7.1* using Colloidal blue staining. Band 16 is pointed by a black arrow. C. a) DHS-3 was examined in LDs of wild type and in four fractions of *dhs-3* deletion mutant using Western blot with anti-DHS-3 (upper panel). Arrow points DHS-3 band. Protein loading was detected by Coomassie blue staining (lower panel). b) LD proteins were compared between wild type and *dhs-3* deletion mutant using Colloidal blue staining. Band 21 is pointed by a black arrow.

30 min at room temperature, and were then denatured at 95 °C for 5 min. The proteins were separated by SDS-PAGE and analyzed using Western blot by a method described in our previous study [30]. Polyclonal antibodies for DHS-3, MDT-28, and F22F7.1 were prepared by AbMax Biotechnology Co., Ltd.

2.4. Mass spectrometry analysis

Lipid droplet proteins were separated on a 10% SDS-PAGE gel and subjected to colloidal-blue staining. The lane with LD proteins was cut into 34 slices. In-gel digestion of each slice was performed as follows: First, the gel was dehydrated with 100% acetonitrile and then the proteins were reduced with 10 mM DTT in 25 mM ammonium bicarbonate at 56 °C for 1 h. The proteins were then alkylated using 55 mM iodoacetamide in 25 mM ammonium bicarbonate in the dark at room temperature for 45 min. Finally, the gel pieces were thoroughly washed with 25 mM ammonium bicarbonate in water–acetonitrile (1:1, v/v) solution and were completely dried in a SpeedVac. Then proteins were incubated with 10 μl trypsin solution (10 ng/μl in 25 mM ammonium bicarbonate) for 30 min on ice. 30–40 μl of 25 mM ammonium bicarbonate was added after removing the excess enzyme solution. 12 hours later, 5% formic acid was added to stop the digestion reaction. A C_{18} trap column was used to capture the peptide solution, which was eluted and then subjected to nano-LC-ESI-LTQ MS/MS analysis. The LTQ mass

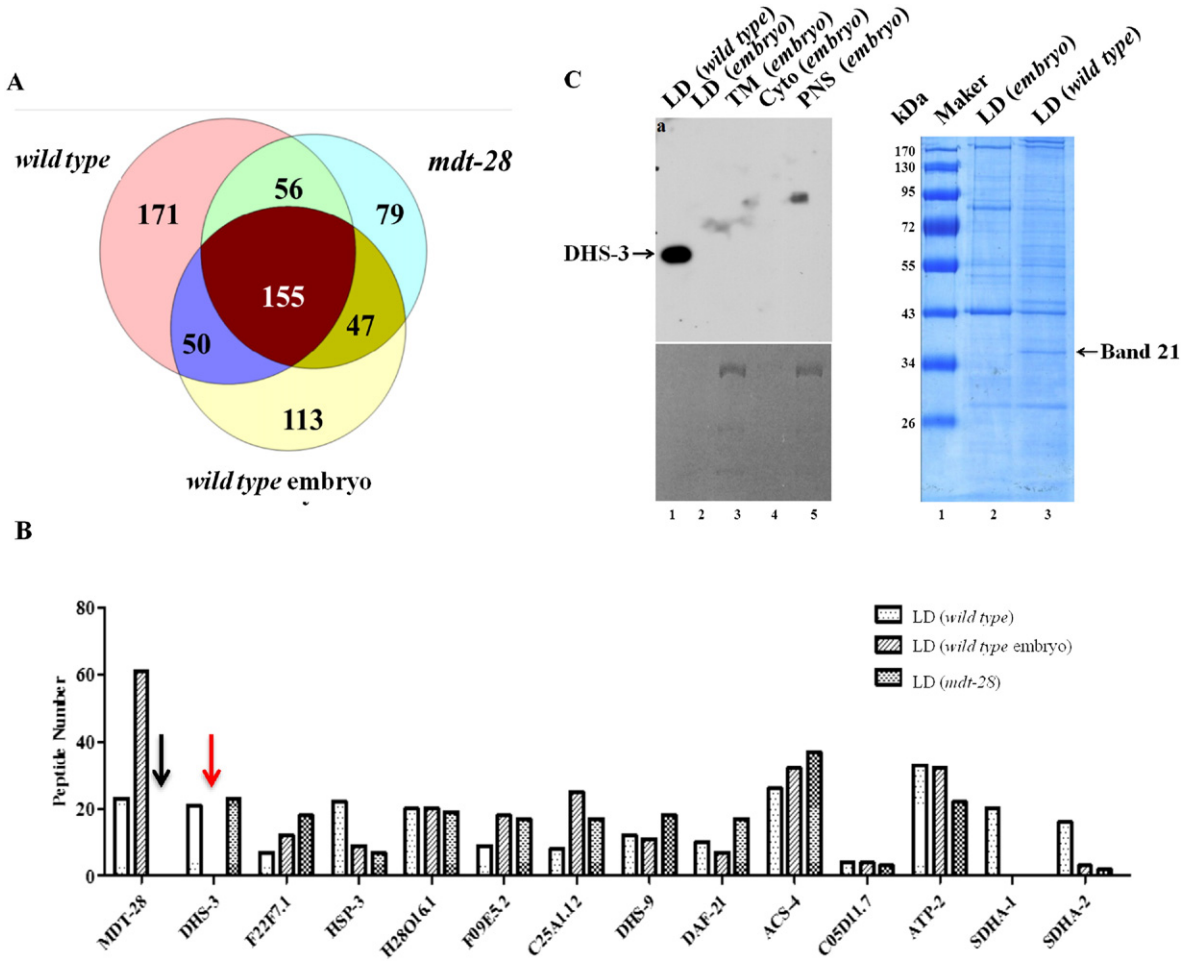

Fig. 3. DHS-3 is not expressed in embryos. A. LDs were isolated from wild type embryos and the LD proteins were subjected to proteomic analysis. The proteomes of the wild type adult and the *mdt-28* mutant were compared. B. The major proteins from proteomes of the wild type adult, the *mdt*-28 mutant adult, and wild type embryos were compared and presented with peptide numbers. C. Analysis by Coomassie blue staining and Western blot of LD proteins from wild type adults and wild type embryos. (a) Upper panel: Specific proteins in cellular fractions were examined by Western blot with polyclonal DHS-3 antibodies; lower panel: Coomassie blue-stained SDS-PAGE as a loading control. (b) LD protein profiles were presented by Colloidal blue-stained SDS-PAGE.

spectrometer was operated under data-dependent mode and was set at an initial 400–2000 Da MS scan range. The five most abundant ions were selected for subsequent collision-activated dissociation. All MS/MS data were searched against the *C. elegans* protein database Wormpep218.

2.5. Lipid droplet targeting sequences of MDT-28 and DHS-3

Following hydrophobicity and secondary structure prediction, DNA coding for DHS-3 was truncated into three fragments coding for amino acids 1–50, 50–150, and 150–307. The fragments and full length of DHS-3 were ligated into EGFP-N1, and were then transfected into CHO K2 cells. After 12 hours, the cells were harvested and fixed with 4% PFA for 30 min, permeabilized with 0.02% Triton X-100 for 8 min, and then stained with LipidTox deep red for 30 min. The prepared samples were examined using confocal microscopy. Similarly, MDT-28 was fragmented into three pieces (coding for 1–210, 210–275, 275–418 amino acids), ligated to EGFP-N1, and then transfected into the CHO K2 cells for fluorescence microscopy.

2.6. Staining and confocal microscopy

For the neutral lipid dye feeding approach, the three dyes (Nile red, Bodipy, LipidTox) were diluted 1:1000 with PBS and 200 μl of the mixture was applied to an OP50 lawn in a Nematode Growth Media (NGM) plate. Then *Pdhs-3::dhs-3::GFP* L4 stage worms were transferred onto the plate. The worms were ready for live image observation after 12 hours.

Fixed Oil Red O and Nile red staining of adult worms was carried out as previously described [29,33]. The stained worms were laid on a 2% agar plate, and then subjected for confocal image analysis. For fixed Bodipy staining of embryos, we used the same protocol as for the fixed Nile red staining of adult worms.

2.7. SRS and fluorescence imaging

Stimulated Raman scattering (SRS) and fluorescence microscopy setup and imaging methods have previously been described [28]. Pump (780 nm–990 nm, tunable) and Stokes (1064 nm) laser beams

Fig. 4. Localization and tissue distribution of primary LD proteins. A. LD localization of DHS-3, MDT-28, and F22F7.1. Transgenic worms with *Pdhs-3::dhs-3::GFP* (a), *Pmdt-28::mdt-28::mcherry* (b), and *PF22F7.1-22::F22F7.1::GFP* (c), respectively, were constructed and then visualized by confocal microscopy as described previously [29]. B. Tissue distribution of MDT-28 and DHS-3. The transgenic animals co-expressing *Pmdt-28::mdt-28::mcherry* and *Pdhs-3::dhs-3::GFP* (a and b were duplicate with different magnification of microscopy), *Pmdt-28::mdt-28::mcherry* and *Pmyo-3::GFP* (c), and *Pmdt-28::mdt-28::mcherry* and *Pceh-14::GFP* (d) were generated and examined using confocal microscopy. C. Transgenic worms expressing *Pdhs-3::dhs-3::GFP* were made and visualized by confocal microscopy as described in the methods. Upper panel: GFP image; lower panel: merged picture of DIC and GFP. Bar = 5 μm.

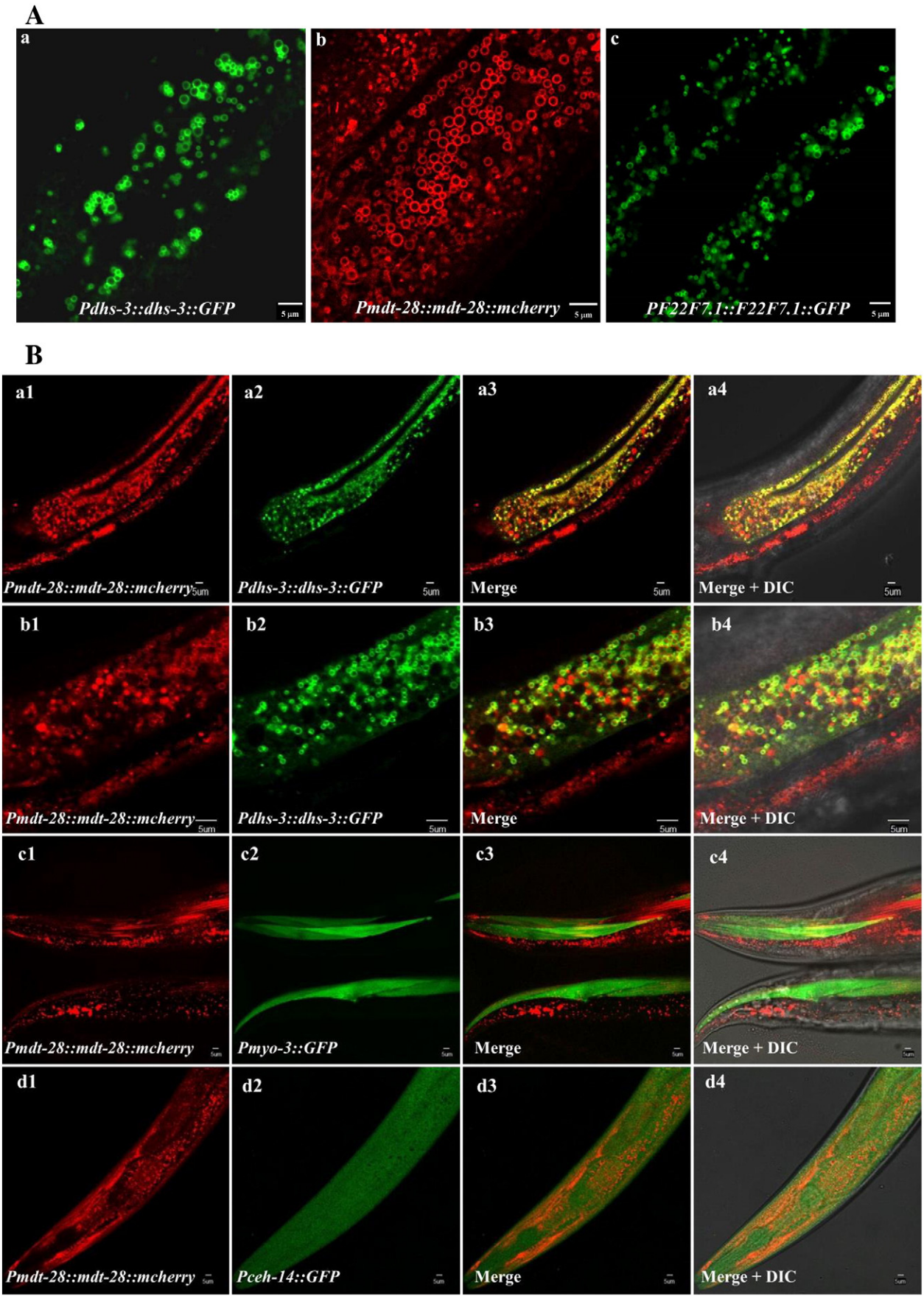
A
a
Pdhs-3::dhs-3::GFP
5 μm
b
Pmdt-28::mdt-28::mcherry
5 μm
c
PF22F7.1::F22F7.1::GFP
5 μm
B
a1
Pmdt-28::mdt-28::mcherry
5um
a2
Pdhs-3::dhs-3::GFP
5um
a3
Merge
5um
a4
Merge + DIC
5um
b1
Pmdt-28::mdt-28::mcherry
5um
b2
Pdhs-3::dhs-3::GFP
5um
b3
Merge
5um
b4
Merge + DIC
5um
c1
Pmdt-28::mdt-28::mcherry
5um
c2
Pmyo-3::GFP
5um
c3
Merge
5um
c4
Merge + DIC
5um
d1
Pmdt-28::mdt-28::mcherry
5um
d2
Pceh-14::GFP
5um
d3
Merge
5um
d4
Merge + DIC
5um

from a *pico*EMERALD one box laser (APE, Germany) were coupled into a modified laser scanning confocal microscope (IX81/FV1000, Olympus) optimized for near-infrared throughput. A 60× water objective (UPlanAPO/IR, 1.2 NA, Olympus) and an oil immersion condenser (NA 1.4, Olympus) were used for high-resolution imaging. GFP fluorescence used a two-photon excited using pump laser at 860 nm, and the fluorescence signal was detected in the backward direction by a PMT with a dichroic beam splitter (FF746-SDi01, Sermrock). Lipid SRS imaging was taken using 816.7 nm pump laser and 1064 nm Stokes laser based on Raman shift of CH2 chemical bonds (2845 cm^{-1}). The GFP images and SRS images were aligned and merged using ImageJ (NIH).

2.8. Mapping identified lipid droplet proteins to Homo sapiens

The analysis reported in Table S2 was performed using the NCBI BLASTP program with default parameters but e-value cutoff set to 1.0E-3. Where more than one gene was mapped, the best hit gene (with lowest BLAST e-value) is listed.

3. Results

3.1. Identification of two most abundant lipid droplet proteins in C. elegans

To identify LD structure-like/resident proteins in *C. elegans*, LDs were isolated from wild type animals. Proteins from the isolated LDs were separated using SDS-PAGE, and were stained using Colloidal blue. The lane with LD proteins was then sliced into 34 pieces corresponding to major stained protein bands. The gel pieces were then subjected to in-gel digestion and the separated peptides were identified using proteomic analysis (Fig. 1A, Table S1) [30]. In total, 154 proteins were identified and classified into 9 categories (Fig. S1, Table S2). Of these, 113 had been previously identified in a study of *C. elegans* LDs (Fig. 1Ba) [29]. Of the proteins found, 87% have been previously identified in isolated LDs from other organisms except *C. elegans* (Fig. 1Bb), which confirms the consistency of the technique with previous studies. To identify LD structure-like/resident proteins in *C. elegans* that are similar to PLIN1 and 2 in mammals, we initially focused on the most abundant proteins of the isolated LDs. The two bands with the highest intensity are marked with red numbers, 16 and 21 in the stained SDS-PAGE (Fig. 1A). To determine the major proteins in these two bands, three replicate LD isolations were conducted and the LD proteins were separated by SDS-PAGE. Bands 16 and 21 were sliced and the proteins determined using proteomic analysis. Three proteins in band 16 (Fig. 1Ca) and six proteins in band 21 (Fig. 1Cb) were identified in all three independent LD isolations. The major protein from band 16 was identified as MDT-28 (Fig. 1Cc), which is a component of the multi-subunit transcriptional mediator complex. Band 21 was dominated by DHS-3 (Fig. 1Cd), which was identified as LD marker protein in a previous study [29].

To verify that MDT-28 was the major protein in band 16 an *mdt-28* deletion mutant (*tm1704* × 4) was obtained and its LDs were isolated. We then compared proteins in the isolated LDs between the *mdt-28* deletion mutant (*tm1704* × 4) (Table S3) and the wild type using comparative proteomics, Western blot analysis, and total protein staining (Fig. 2A). The LD proteins from the wild type animals were analyzed by Western blot using a polyclonal antibody against MDT-28, generated by ABMAX. MDT-28 was detected in the LD fraction but not in other cellular fractions such as the cytosol (Cyto), total membrane (TM), and post-nuclear supernatant (PNS), suggesting that MDT-28 is a LD resident protein (Fig. 2Aa, lanes 2 to 5). When the quantity of PNS proteins was increased 10-fold or 50-fold (as represented by protein staining) (Fig. 2Aa, lower panel, lanes 6 and 7), MDT-28 could be detected in PNS (Fig. 2Aa, lane 7).

As expected, no MDT-28 signal was detected in the mutant LDs by Western blot analysis (Fig. 2Aa, lane 1 and arrow), confirming the deletion of the protein. An examination of the stained SDS-PAGE also reveals that band 16 was absent from isolated LDs of the *mdt-28* deletion mutant (Fig. 2Ab, lane 3 and arrow). This verifies that band 16 primarily consisted of MDT-28 protein, in agreement with the proteomic result (Fig. 1Cc). However, a new band also appeared in the mutant LDs, having a slightly higher molecular weight than MDT-28 (Fig. 2Ab, lane 3 and red arrow). The band was sliced from the gel and subjected to a proteomic analysis. This protein was identified as F22F7.1, which was confirmed by Western blot (Fig. 2Ba, lanes 2 to 7). Interestingly, Western blot also demonstrated in substantial increase in the quantity of F22F7.1 in *mdt-28* deletion mutant LDs, compared with the wild type (Fig. 2Ba, compare lane 1 to 2 and arrow), in agreement with data presented in Figs. 1C, 2Ab in lane 3, and 2Bb in lane 3.

Based on sequence similarity, F22F7.1 is similar to CGI-49, a mammalian LD protein (Fig. S3a), suggesting that F22F7.1 (CGI-49) functions as a redundant protein of MDT-28. Thus, we acquired the F22F7.1 deletion mutant to determine if there were other major proteins in the band. Since MDT-28 and F22F7.1 have similar molecular weights we crossed the two knockouts to produce a double mutant. LDs were then isolated from the double deletion mutant, the proteins were separated using SDS-PAGE, and were then stained with Colloidal blue. Neither the MDT-28 nor the F22F7.1 containing bands were present, indicating that F22F7.1 made up the majority of the new band (Fig. 2Bb, lane 3 and arrow). Together, these data demonstrate that MDT-28 is main resident protein of *C. elegans* LDs, and F22F7.1 is significantly increased on LDs following MDT-28 deletion.

We then sought to identify the major protein of the second prominent band, marked as band 21 (~36 kDa) (Fig. 1A). We back-crossed the *dhs-3* deletion mutant (gk873395) against the wild type six times and then isolated LDs. We compared the protein patterns of the mutant and wild type by Colloidal blue staining and Western blot. The knockout of DHS-3 in the *dhs-3* mutant was confirmed by Western blot (Fig. 2Ca, lane 2 and arrow). Band 21 was barely detectable in the stained SDS-PAGE of the *dhs-3* deletion mutant (Fig. 2Cb, lane 3 and arrow). These results verified that band 21 mainly consisted of DHS-3 protein, which is consistent with the proteomic data (Fig. 1Cd).

Next, to provide LD proteome for study of lipid metabolism during the development of *C. elegans*, we purified LDs from isolated embryos (Fig. S2 and Table S4) [32] and conducted a shotgun proteomic analysis (Table S4). We then compared this proteome with that from young adults of wild type and also the *mdt-28* deletion mutant, and observed that 154 proteins were common to all three proteomes (Fig. 3A). By comparing all three proteomes based on their peptide numbers, we also revealed that there was a higher expression of MDT-28 and C25A1.12 (CGI-58 based on sequence similarity) in the embryonic LDs (Fig. 3B), and lower expression of HSP-3, succinate dehydrogenase complex, subunit A-1 and 2 (SDHA-1 and SDHA-2) in both *mdt-28* mutant and embryonic LDs (Fig. 3B). Interestingly, we found that DHS-3 was absent in embryonic LD proteome (Fig. 3B and red arrow).

We then performed Western blot analysis to verify the proteomic results. It was clear that no DHS-3 signal was detected in embryonic LD proteins (Fig. 3Ca, lane 2 and arrow). DHS-3 could not be detected in other cellular fractions either, suggesting that DHS-3 was not expressed in embryos (Fig. 3Ca, lanes 3–5). This was consistent with the absence of band 21 in Coomassie stained gels proteins from the embryonic LDs (Fig. 3Cb, lane 2). Thus, using proteomic and biochemical studies, we identified the two most abundant proteins of *C. elegans* LDs, MDT-28 and DHS-3.

3.2. Location of MDT-28, DHS-3, and F22F7.1

To examine the physiological location of DHS-3, MDT-28, and F22F7.1 in *C. elegans*, we performed a morphological analysis. Initially, we generated transgenic animals with *Pmdt-28::mdt-28::mCherry*, *Pdhs-3::dhs-3::GFP*, and *PF22F7.1::F22F7.1::GFP*, and observed the cellular localization of these fusion proteins within the living animals using confocal microscopy. DHS-3 (Fig. 4Aa), MDT-28 (Fig. 4Ab), and F22F7.1 (Fig. 4Ac), were mainly present on ring-like structures,

suggesting that they were surrounding LDs, verifying the results from proteomic and biochemical studies.

To determine the location of these proteins under lower expression levels, transgenic animals carrying a single copy of the transgenes; *Pvha-6::dhs-3::GFP* and *Pmdt-28::mdt-28::mRuby* were also generated and examined using confocal microscopy. As before, ring structures of the DHS-3 and MDT-28 fusion proteins were seen in the transgenic animals, further confirming the LD location of these two proteins (Fig. S2a and b). These results, combined with our proteomic and biochemical data, suggest that MDT-28 and DHS-3 are LD resident proteins of *C. elegans*.

3.3. Tissue distribution and lipid droplet targeting of MDT-28 and DHS-3

After confirming the LD location of MDT-28, DHS-3, and F22F7.1, we then proceeded to determine their tissue distributions. We focused on MDT-28 and DHS-3, since they were the two most abundant LD resident proteins of *C. elegans*. *C. elegans* strains expressing *Pmdt-28::mdt-28::mCherry* and *Pdhs-3::dhs-3::GFP* were crossed to generate a double fluorescent animal. When the animal was examined, we observed that all GFP signalswere co-localized with the mCherry signal. However, some mCherry signal was independent of the GFP (Fig. 4Ba3 and Bb3).

Based on the morphology, the DHS-3 seemed to be mainly localized on intestinal LDs. To determine the tissue distribution of the MDT-28 which was not overlapping with GFP signals, we crossed *Pmdt-28::mdt-28::mCherry* with strains expressing muscle specific *Pmyo-3::GFP* (Fig. 4Bc2) [34] and hypodermis specific *Pceh-14::GFP* (Fig. 4Bd2) [35]. We observed co-localizing fluorescence of mCherry and GFP in both (Fig. 4Bc3 and Bd3), suggesting a distribution of MDT-28 in the muscle and hypodermis. Moreover, in agreement with the proteomic and biochemical results (Fig. 3B and C), DHS-3::GFP was not detected in the embryos, but interestingly was found in the vulva of adults (Fig. 4C).

To further characterize MDT-28 and DHS-3 as LD resident proteins of *C. elegans*, their LD targeting mechanisms were examined. Truncation mutations based on their hydrophobicity profiles and potential α-helices (Fig. 5Aa, Ab) were constructed and fused with GFP. The truncated GFP fusion proteins were expressed in Chinese hamster ovary (CHO K2) cells, and their cellular localization examined using confocal microscopy.

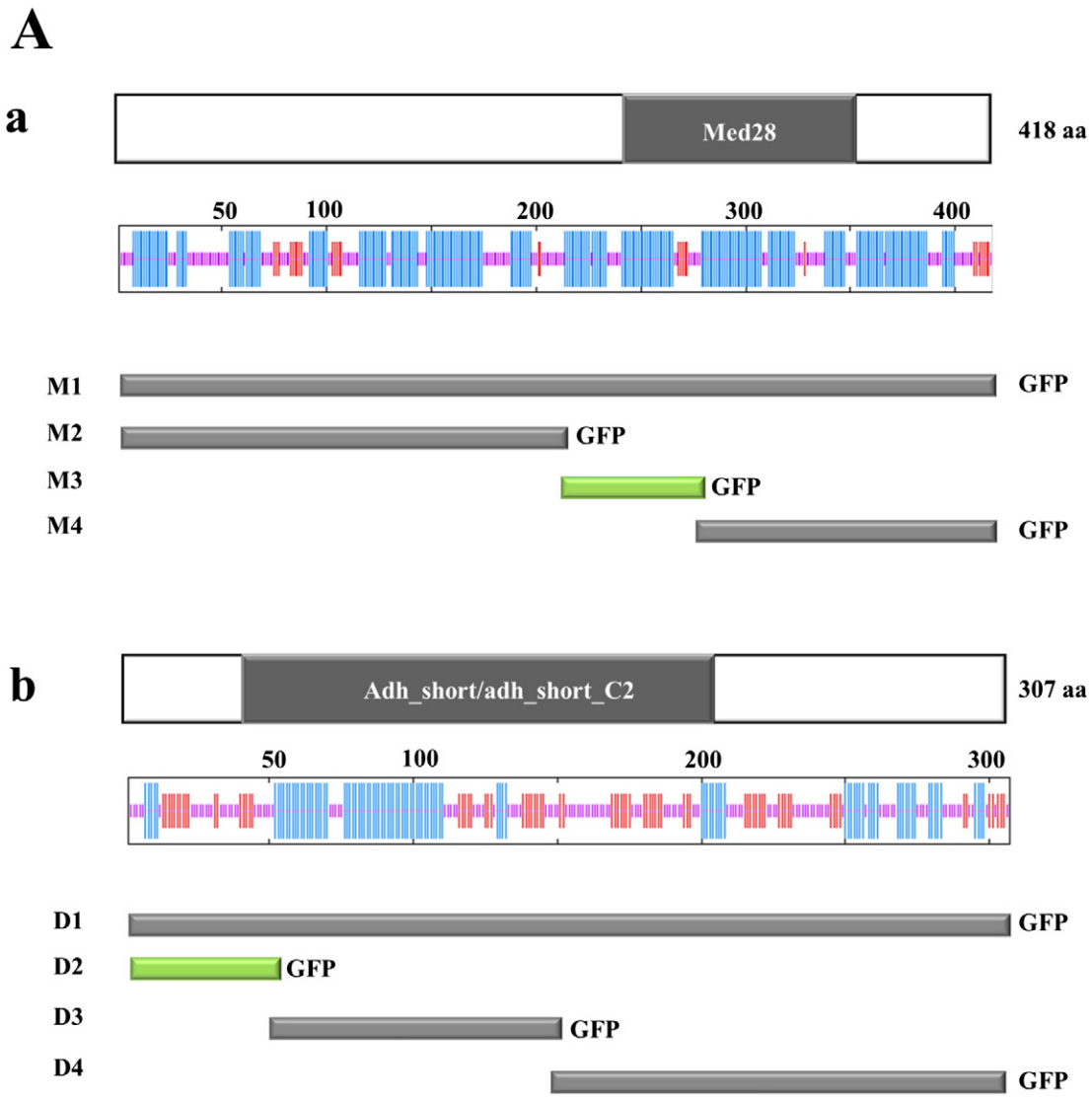

Fig. 5. LD targeting of MDT-28 and DHS-3. A. Truncations of MDT-28 (a) and DHS-3 (b) were made based on hydrophobicity (indicated with red vertical lines) and potential alpha helices (indicated with blue vertical lines). B–C. Truncated proteins were fused with GFP, expressed in Chinese hamster ovary (CHO K2) cells, and co-imaged with LipidTox staining using confocal microscopy. The truncated *MDT-28::GFP* fragments M1, M2, M3, M4 are shown in with M1 to M4, respectively and the *DHS-3::GFP* fragments D1, D2, D3, D4 are shown in with D1 to D4, respectively. G represents GFP. Bar = 2 μm.

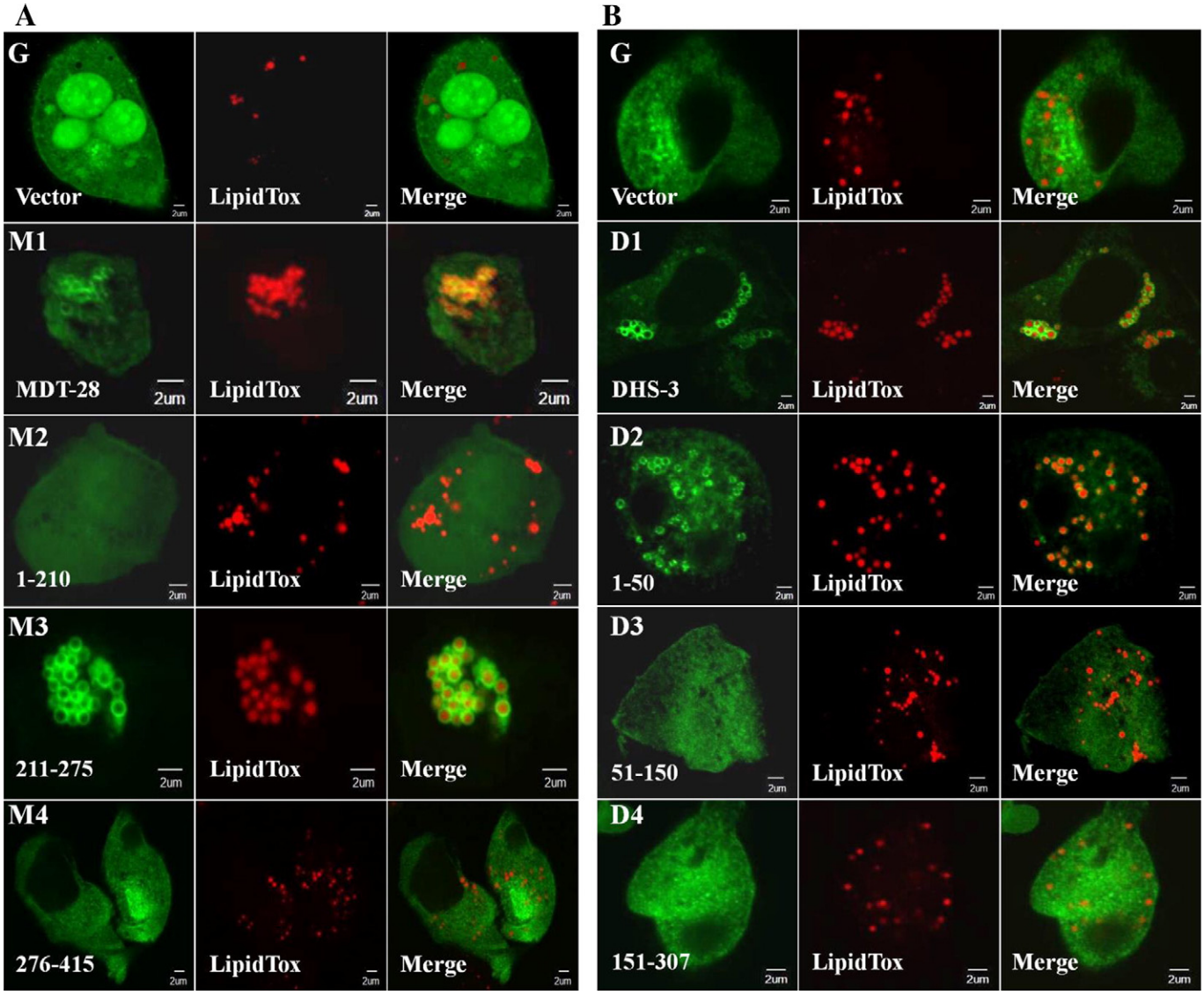

Fig. 5 (*continued*).

In addition to the LD localization of the full length proteins (Fig. 5B-M1 and C-D1), truncation mutants containing amino acids 211 through 275 of MDT-28 (Fig. 5B-M3) and 1 through 50 of DHS-3 (Fig. 5C-D2) formed ring structures around LipidTox-stained LDs in CHO K2 cells. Other fragments of two proteins were detected in the cytosol, and none of these fragments were found on other membrane structures. These results not only identified the protein region of MDT-28 and DHS-3 responsible for LD targeting but also provide further confirmation that these are LD proteins.

Lacking confirmed LD marker proteins, the study of this organelle in *C. elegans* has depended on several lipid dyes. These lipid dyes, such as Oil Red O, Nile red, boron-dipyrromethene (Bodipy), and LipidTox have facilitated lipid research in *C. elegans* but have also been found to be problematic, as previously reported [27,28,36]. Using the newly verified LD resident protein DHS-3::GFP we examined whether these dyes stained LDs in *C. elegans*. We either fed the transgenic worm, *Pdhs-3::dhs-3::GFP* with these dyes or fixed the transgenic worm then stained them with these dyes. It was clear that the fluorescence introduced by feeding the animals Nile red (Fig. 6Aa3) and LipidTox (Fig. 6Ac3) did not co-localize with DHS-3::GFP. Some weak signal from feeding Bodipy was localized inside of the DHS-3::GFP rings (Fig. 6Ae3). In contrast, the use of all four dyes post-fixation gave signals that were well co-localized with DHS-3::GFP (Fig. 6Ab3, Ad3, Af3, and Ag3).

To overcome the limitations associated with lipid staining, especially the requirement for the fixation of the animals, methods using coherent anti-Stokes Raman scattering (CARS) microscopy [37] and stimulated Raman scattering (SRS) microscopy [28] were established using living animals. We then used DHS-3::GFP to determine whether the SRS signal detected represented LDs in the animal. When strain *Pdhs-3::dhs-3::GFP* was visualized by SRS microscopy the SRS signal was almost entirely located inside of DHS-3::GFP ring structures, suggesting that the SRS signals indeed represented *C. elegans* LDs (Fig. 6B).

3.4. dhs-3 and mdt-28 regulate lipid droplet phenotype

Since MDT-28 and DHS-3 are the two major resident proteins of C. elegans LDs, it is necessary to determine their functions, including their effects on LD morphological regulation. Wild type and *dhs-3* mutant worms were fixed and stained with Nile red (Fig. 7Aa and Ab), and the images quantified for LD size. The results show a clear decrease in LD size in the *dhs-3* mutant (Fig. 7Ba). There was also a notable reduction in TAG content in the *dhs-3* mutant (Fig. 7Bb), suggesting that DHS-3 is essential to maintain LD size and TAG content.

We then examined the effect of MDT-28 on the organelle including LD numbers and size. To do so, we generated a *dhs-3* single copy transgenic worm with an intestinal specific promoter, *Pvha-6::dhs-3::GFP*

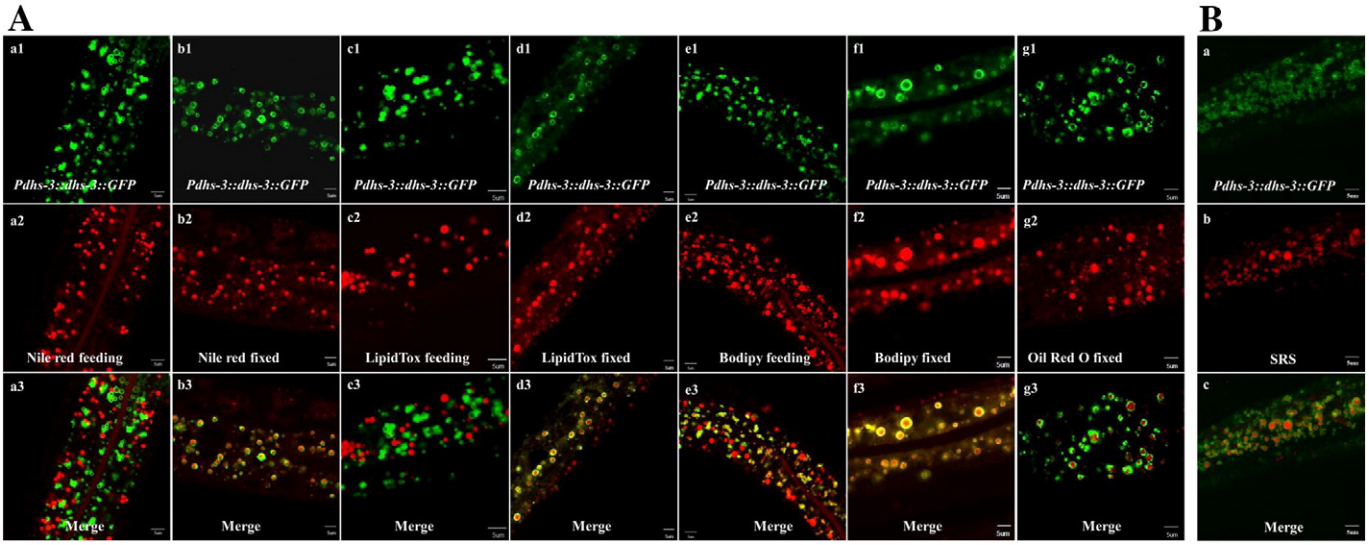

Fig. 6. Comparison with other lipid droplet staining methods. A. *Pdhs-3::dhs-3::GFP* strain was stained with commercial neutral lipid dyes by either feeding or labeling after fixation, and examined using confocal microscopy. B. *Pdhs-3::dhs-3::GFP* worms were imaged using stimulated Raman scattering (SRS) microscopy [28]. DHS-3::GFP image was taken by two-photon excited fluorescence mode. The corresponding lipid SRS image of the same area was taken using SRS based on CH2 chemical bonds. Bar = 5 μm.

(Fig. 7Ca) and crossed it with *mdt-28* (Fig. 7Cb). The *mdt-28* deletion mutation resulted in clustered LDs (Fig. 7Cb and Da). The clustering could be rescued by fosmid WRM0612Df08 (Fig. 7Cc). The *mdt-28* mutation resulted in a slightly reduced TAG level in *C. elegans* (Fig. 7Db). Together, the data suggest that, compared with DHS-3, MDT-28 plays a less important role in maintaining LD TAG content, but it does appear to protect LDs from aggregation that may be an initiating step of in LD fusion.

4. Discussion

This comparative proteomic study of LDs from wild type and mutant *C. elegans*, combined with biochemical experiments with novel antibodies, provides a systematic analysis of LD-associated proteins in the worm. Chief among the findings is the identification of two structure-like/resident proteins, DHS-3 and MDT-28, that have a clear phenotype when knocked out, confirming their centrality to LD structure and function. Collectively, the results presented here provide a roadmap for future mechanistic research into lipid storage and metabolism in this important genetic model.

In mammalian cells, PLIN1 and PLIN2 are LD structure-like/resident proteins [38] that are almost exclusively located on LDs. Previous studies have not only utilized them as marker proteins but have also revealed that these two proteins play essential roles in the storage and mobilization of cellular neutral lipids. Unfortunately, no PLIN family proteins have been found in *C. elegans*, limiting the use of this animal in study of lipid metabolism.

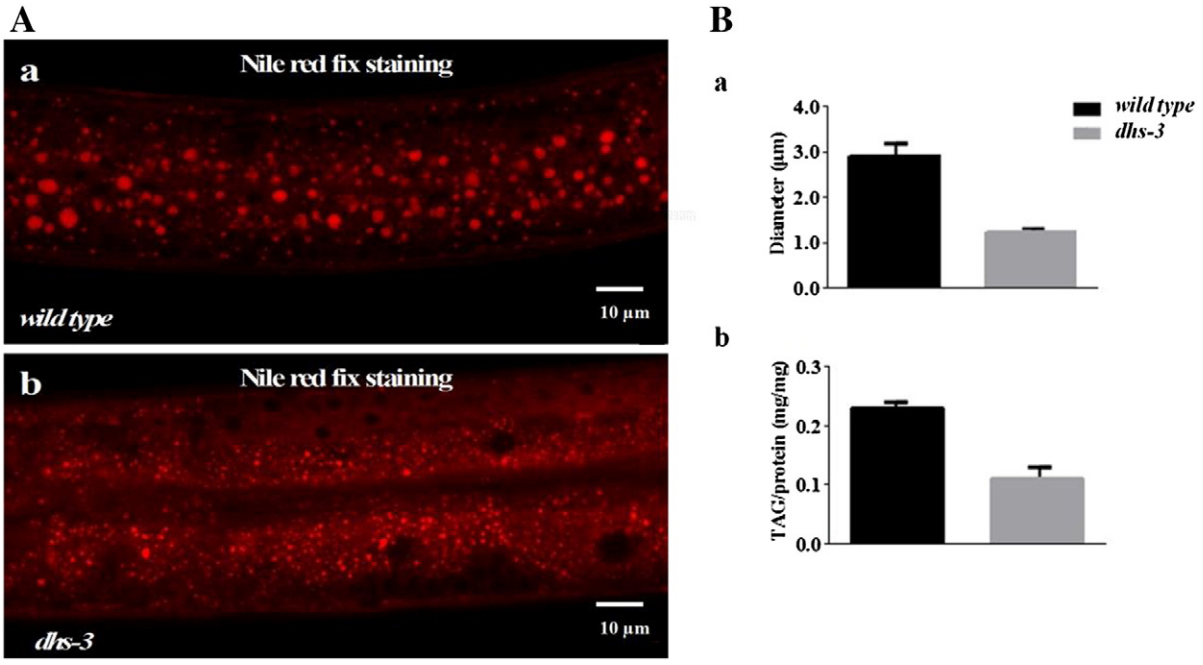

Fig. 7. *dhs-3* and *mdt-28* regulated lipid droplet morphology. A. L4 worms of wild type strain (a) and *dhs-3* mutant strain (b) were fixed and stained with Nile red. Bar = 10 μm. B. The diameter of stained LDs (a) and TAG content/total proteins (b) were quantified. C. L4 worms of the wild type strain (a), *mdt-28* deletion mutant (b), and *mdt-28* rescued strain (c) were crossed with *Pvha-6::dhs-3::GFP* and examined by fluorescence microscopy. D. The degree of LD clustering (a) and TAG content/total proteins (b) were quantified. Bar = 5 μm.

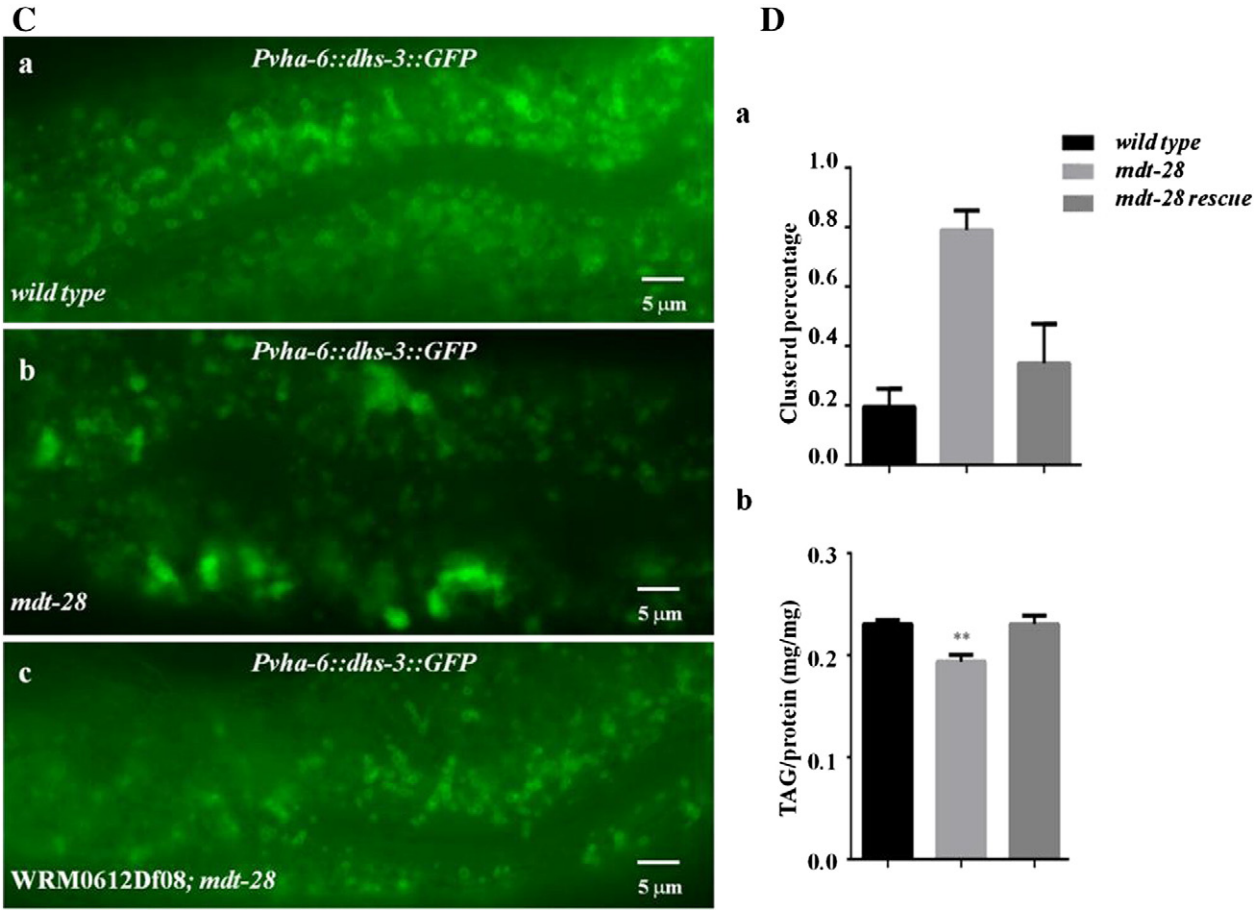

Fig. 7 (*continued*).

In the present work, we identified the two most abundant proteins in *C. elegans* LDs, DHS-3 and MDT-28, and confirmed their LD location using proteomic, biochemical and morphological studies (Figs. 2 and 3). In addition, we determined the regions of these proteins responsible for their LD targeting (Fig. 4). The *dhs-3* and *mdt-28* mutants had clear phenotypes in LD size, TAG content and clustering (Fig. 7) possibly linking them with the functional role mammalian PLIN1 and PLIN2 in protecting LD TAG from lipolysis. Based on the observation that these proteins are abundant (main bands) (Figs. 1 and 2), restricted to LDs (Figs. 2, 3 and 4), and have roles in regulating LD size, TAG content, and clustering (Fig. 7), we conclude that DHS-3 and MDT-28 are LD structure-like/resident proteins in *C. elegans*, similar to PLIN family proteins in mammalian cells.

Having identified DHS-3, MDT-28, and F22F7.1, another LD protein of note, we searched for mammalian homologues based on amino acid sequence similarity. As shown in the domain composition map in Fig. 5Aa, MDT-28 contains a MED-28 (mediator complex subunit 28, mediator of RNA polymerase II, transcriptional regulator) domain. An adh_short (short chain dehydrogenase) domain was found in DHS-3, indicating similarity to 17βHSD11. Many short chain dehydrogenase/reductase (SDR) family proteins are associated to LDs and involved in lipid metabolism, including 17βHSD2, 17βHSD7, 17βHSD11, 17βHSD13, 3βHSD1, DHRS3[8,39–43]. Finally, F22F7.1 is similar to CGI-49, another mammalian LD protein (Fig. S3a).

Our data suggest that MDT-28 is a ubiquitously distributed LD protein similar to that of ADRP/PLIN2 [10] while DHS-3 is more like a single-tissue expressed LD protein like PLIN1 [15] in mammals. The distinct tissue distributions of DHS-3 and MDT-28 (Fig. 4B) demonstrate the heterogeneity of LDs in the animal, which may prove useful in determining the breadth of functional roles LDs play in an organism. Furthermore, with these two newly identified LD resident proteins, it becomes possible to search for genes governing lipid storage in specific tissues of *C. elegans* by RNAi screening. The discovery that F22F7.1 was increased in LDs when MDT-28 was deleted (Fig. 2), suggests that F22F7.1 may provide functional redundancy with MDT-28. This observation may provide a clue to uncover the function of the homologous CGI-49 in mammalian cells.

In conclusion, this work provides a molecular basis for future research into fat storage and metabolism in *C. elegans* and further establishes *C. elegans* as a powerful model for the study of lipid storage-related disease states.

Conflict of interest

All authors disclosed no conflicts of financial and other interests.

Acknowledgements

The authors thank Dr. John Zehmer for his critical reading and useful suggestions. The authors also thank the *Caenorhabditis* Genome Center (CGC) and National BioResource Project (NBRP) for providing strains. This work was supported by grant 2011CBA00906 from the Ministry of Science and Technology of China and grants from the National Natural Science Foundation of China (No. 31000365, No. 61273228, No. 81270932).

Appendix A. Supplementary data

Supplementary data to this article can be found online at http://dx.doi.org/10.1016/j.bbamcr.2015.05.020.

References

[1] D.J. Murphy, The biogenesis and functions of lipid bodies in animals, plants and microorganisms, Prog. Lipid Res. 40 (2001) 325–438.
[2] S. Martin, R.G. Parton, Lipid droplets: a unified view of a dynamic organelle, Nat. Rev. Mol. Cell Biol. 7 (2006) 373–378.
[3] N.A. van Herpen, V.B. Schrauwen-Hinderling, Lipid accumulation in non-adipose tissue and lipotoxicity, Physiol. Behav. 94 (2008) 231–241.
[4] R.V. Farese Jr., T.C. Walther, Lipid droplets finally get a little R-E-S-P-E-C-T, Cell 139 (2009) 855–860.
[5] L. Yang, Y. Ding, Y. Chen, S. Zhang, C. Huo, Y. Wang, J. Yu, P. Zhang, H. Na, H. Zhang, Y. Ma, P. Liu, The proteomics of lipid droplets: structure, dynamics, and functions of the organelle conserved from bacteria to humans, J. Lipid Res. 53 (2012) 1245–1253.
[6] D.J. Murphy, The dynamic roles of intracellular lipid droplets: from archaea to mammals, Protoplasma 249 (2012) 541–585.
[7] R. Bartz, W.H. Li, B. Venables, J.K. Zehmer, M.R. Roth, R. Welti, R.G. Anderson, P. Liu, K.D. Chapman, Lipidomics reveals that adiposomes store ether lipids and mediate phospholipid traffic, J. Lipid Res. 48 (2007) 837–847.
[8] P. Liu, Y. Ying, Y. Zhao, D.I. Mundy, M. Zhu, R.G. Anderson, Chinese hamster ovary K2 cell lipid droplets appear to be metabolic organelles involved in membrane traffic, J. Biol. Chem. 279 (2004) 3787–3792.
[9] A.S. Greenberg, J.J. Egan, S.A. Wek, N.B. Garty, E.J. Blanchette-Mackie, C. Londos, Perilipin, a major hormonally regulated adipocyte-specific phosphoprotein associated with the periphery of lipid storage droplets, J. Biol. Chem. 266 (1991) 11341–11346.
[10] H.P. Jiang, G. Serrero, Isolation and characterization of a full-length cDNA coding for an adipose differentiation-related protein, Proc. Natl. Acad. Sci. U. S. A. 89 (1992) 7856–7860.
[11] D.L. Brasaemle, T. Barber, N.E. Wolins, G. Serrero, E.J. Blanchette-Mackie, C. Londos, Adipose differentiation-related protein is an ubiquitously expressed lipid storage droplet-associated protein, J. Lipid Res. 38 (1997) 2249–2263.
[12] N.E. Wolins, B. Rubin, D.L. Brasaemle, TIP47 associates with lipid droplets, J. Biol. Chem. 276 (2001) 5101–5108.
[13] N.E. Wolins, J.R. Skinner, M.J. Schoenfish, A. Tzekov, K.G. Bensch, P.E. Bickel, Adipocyte protein S3-12 coats nascent lipid droplets, J. Biol. Chem. 278 (2003) 37713–37721.
[14] N.E. Wolins, B.K. Quaynor, J.R. Skinner, A. Tzekov, M.A. Croce, M.C. Gropler, V. Varma, A. Yao-Borengasser, N. Rasouli, P.A. Kern, B.N. Finck, P.E. Bickel, OXPAT/PAT-1 is a PPAR-induced lipid droplet protein that promotes fatty acid utilization, Diabetes 55 (2006) 3418–3428.
[15] A.R. Kimmel, D.L. Brasaemle, M. McAndrews-Hill, C. Sztalryd, C. Londos, Adoption of PERILIPIN as a unifying nomenclature for the mammalian PAT-family of intracellular lipid storage droplet proteins, J. Lipid Res. 51 (2010) 468–471.
[16] S. Ozeki, J. Cheng, K. Tauchi-Sato, N. Hatano, H. Taniguchi, T. Fujimoto, Rab18 localizes to lipid droplets and induces their close apposition to the endoplasmic reticulum-derived membrane, J. Cell Sci. 118 (2005) 2601–2611.
[17] S. Martin, K. Driessen, S.J. Nixon, M. Zerial, R.G. Parton, Regulated localization of Rab18 to lipid droplets: effects of lipolytic stimulation and inhibition of lipid droplet catabolism, J. Biol. Chem. 280 (2005) 42325–42335.
[18] P.S. Liu, R. Bartz, J.K. Zehmer, Y.S. Ying, M. Zhu, G. Serrero, R.G.W. Anderson, Rab-regulated interaction of early endosomes with lipid droplets, Biochim. Biophys. Acta, Mol. Cell Res. 1773 (2007) 784–793.
[19] J. Pu, C.W. Ha, S. Zhang, J.P. Jung, W.K. Huh, P. Liu, Interactomic study on interaction between lipid droplets and mitochondria, Protein Cell 2 (2011) 487–496.
[20] D. Binns, T. Januszewski, Y. Chen, J. Hill, V.S. Markin, Y. Zhao, C. Gilpin, K.D. Chapman, R.G. Anderson, J.M. Goodman, An intimate collaboration between peroxisomes and lipid bodies, J. Cell Biol. 173 (2006) 719–731.
[21] J.K. Zehmer, Y. Huang, G. Peng, J. Pu, R.G. Anderson, P. Liu, A role for lipid droplets in inter-membrane lipid traffic, Proteomics 9 (2009) 914–921.
[22] C. Kenyon, J. Chang, E. Gensch, A. Rudner, R. Tabtiang, A C. elegans mutant that lives twice as long as wild type, Nature 366 (1993) 461–464.
[23] T.J. Brock, J. Browse, J.L. Watts, Fatty acid desaturation and the regulation of adiposity in Caenorhabditis elegans, Genetics 176 (2007) 865–875.
[24] M.C. Wang, E.J. O'Rourke, G. Ruvkun, Fat metabolism links germline stem cells and longevity in *C. elegans*, Science 322 (2008) 957–960.
[25] H.Y. Mak, Lipid droplets as fat storage organelles in *Caenorhabditis elegans*: thematic review series: lipid droplet synthesis and metabolism: from yeast to man, J. Lipid Res. 53 (2012) 28–33.
[26] R.M. McKay, J.P. McKay, L. Avery, J.M. Graff, *C. elegans*: a model for exploring the genetics of fat storage, Dev. Cell 4 (2003) 131–142.
[27] E.J. O'Rourke, A.A. Soukas, C.E. Carr, G. Ruvkun, *C. elegans* major fats are stored in vesicles distinct from lysosome-related organelles, Cell Metab. 10 (2009) 430–435.
[28] M.C. Wang, W. Min, C.W. Freudiger, G. Ruvkun, X.S. Xie, RNAi screening for fat regulatory genes with SRS microscopy, Nat. Methods 8 (2011) 135–138.
[29] P. Zhang, H. Na, Z. Liu, S. Zhang, P. Xue, Y. Chen, J. Pu, G. Peng, X. Huang, F. Yang, Z. Xie, T. Xu, P. Xu, G. Ou, S.O. Zhang, P. Liu, Proteomic study and marker protein identification of *Caenorhabditis elegans* lipid droplets, Mol. Cell. Proteomics MCP 11 (2012) 317–328.
[30] R. Bartz, J.K. Zehmer, M. Zhu, Y. Chen, G. Serrero, Y. Zhao, P. Liu, Dynamic activity of lipid droplets: protein phosphorylation and GTP-mediated protein translocation, J. Proteome Res. 6 (2007) 3256–3265.
[31] Y.F. Ding, S.Y. Zhang, L. Yang, H.M. Na, P. Zhang, H.N. Zhang, Y. Wang, Y. Chen, J.H. Yu, C.X. Huo, S.M. Xu, M. Garaiova, Y.S. Cong, P.S. Liu, Isolating lipid droplets from multiple species, Nat. Protoc. 8 (2013) 43–51.
[32] C.J. Thorpe, A. Schlesinger, J.C. Carter, B. Bowerman, Wnt signaling polarizes an early C. elegans blastomere to distinguish endoderm from mesoderm, Cell 90 (1997) 695–705.
[33] H. Zhang, Y. Wang, J. Li, J. Yu, J. Pu, L. Li, H. Zhang, S. Zhang, G. Peng, F. Yang, P. Liu, Proteome of skeletal muscle lipid droplet reveals association with mitochondria and apolipoprotein a-I, J. Proteome Res. 10 (2011) 4757–4768.
[34] H. Kuroyanagi, T. Kobayashi, S. Mitani, M. Hagiwara, Transgenic alternative-splicing reporters reveal tissue-specific expression profiles and regulation mechanisms in vivo, Nat. Methods 3 (2006) 909–915.
[35] G. Cassata, H. Kagoshima, Y. Andachi, Y. Kohara, M.B. Durrenberger, D.H. Hall, T.R. Burglin, The LIM homeobox gene ceh-14 confers thermosensory function to the AFD neurons in *Caenorhabditis elegans*, Neuron 25 (2000) 587–597.
[36] K. Ashrafi, F.Y. Chang, J.L. Watts, A.G. Fraser, R.S. Kamath, J. Ahringer, G. Ruvkun, Genome-wide RNAi analysis of Caenorhabditis elegans fat regulatory genes, Nature 421 (2003) 268–272.
[37] T. Hellerer, C. Axang, C. Brackmann, P. Hillertz, M. Pilon, A. Enejder, Monitoring of lipid storage in *Caenorhabditis elegans* using coherent anti-Stokes Raman scattering (CARS) microscopy, Proc. Natl. Acad. Sci. U. S. A. 104 (2007) 14658–14663.
[38] D.L. Brasaemle, Thematic review series: adipocyte biology. The perilipin family of structural lipid droplet proteins: stabilization of lipid droplets and control of lipolysis, J. Lipid Res. 48 (2007) 2547–2559.
[39] Y. Fujimoto, H. Itabe, J. Sakai, M. Makita, J. Noda, M. Mori, Y. Higashi, S. Kojima, T. Takano, Identification of major proteins in the lipid droplet-enriched fraction isolated from the human hepatocyte cell line HuH7, Biochim. Biophys. Acta 1644 (2004) 47–59.
[40] K. Athenstaedt, D. Zweytick, A. Jandrositz, S.D. Kohlwein, G. Daum, Identification and characterization of major lipid particle proteins of the yeast Saccharomyces cerevisiae, J. Bacteriol. 181 (1999) 6441–6448.
[41] J. Bouchoux, F. Beilstein, T. Pauquai, I.C. Guerrera, D. Chateau, N. Ly, M. Alqub, C. Klein, J. Chambaz, M. Rousset, J.M. Lacorte, E. Morel, S. Demignot, The proteome of cytosolic lipid droplets isolated from differentiated Caco-2/TC7 enterocytes reveals cell-specific characteristics, Biol. Cell. 103 (2011) 499–517.
[42] F. Beilstein, J. Bouchoux, M. Rousset, S. Demignot, Proteomic analysis of lipid droplets from Caco-2/TC7 enterocytes identifies novel modulators of lipid secretion, PLoS One 8 (2013) e53017.
[43] W. Su, Y. Wang, X. Jia, W. Wu, L. Li, X. Tian, S. Li, C. Wang, H. Xu, J. Cao, Q. Han, S. Xu, Y. Chen, Y. Zhong, X. Zhang, P. Liu, J.A. Gustafsson, Y. Guan, Comparative proteomic study reveals 17beta-HSD13 as a pathogenic protein in nonalcoholic fatty liver disease, Proc. Natl. Acad. Sci. U. S. A. 111 (2014) 11437–11442.